
Measurement of energy spread near $\Lambda_c^+\bar{\Lambda}_c^-$ production threshold

Dong Liu^a, Weiping Wang^a, Baldini Ferroli Rinaldo^{b,c}, Guangshun Huang^a,

^a USTC, Hefei, PRC

^b IHEP, Beijing, PRC

^c INFN-LNF, Frascati, Italy

Abstract Two methods of energy spread measurement are introduced based on threshold truncation effect and spectrum resolution, which are verified with the $e^+e^- \rightarrow \Lambda_c^+\bar{\Lambda}_c^-$ process using BESIII data. The energy spreads obtained with Monte Carlo are reasonable as expected as the extrapolation of that measured at J/ψ resonance. The methods can be alternative options to estimate energy spread.

Key words beam energy spread, production threshold, $\Lambda_c^+\bar{\Lambda}_c^-$ pair, spectrum resolution

PACS

1 Introduction

Precision measurements in high-energy, nuclear, and accelerator physics are vital for the continuous progress in these fields of science. For accelerator based experiments in particular, the precise knowledge of the beam energy E_{beam} is extremely important in order to achieve the highest possible accuracy of the derived parameters. The accuracy of beam energy results from intrinsic and technical reasons, e.g. quantum emission, space charge effect, Touschek effect, synchrotron radiation, etc. Energy spread σ_E is one of the parameters to describe the accuracy, whose exact value enables us to reduce significantly a systematical error in precision measurement. For example, energy spread can help to obtain a reasonable radiation correction factor and efficiency in the cross section measurement of hadron pair production near threshold, e.g. $e^+e^- \rightarrow \Lambda_c^+\bar{\Lambda}_c^-$ at 4575 MeV.

In principle, every variable sensitive to σ_E can be used for the energy spread measurement, although not all parameters are equally suited. There are several methods to measure σ_E . In accelerator, spectrum of chromatic sideband peak of beam betatron oscillation is related to energy spread. Thus, σ_E can be determined on basis of the measurement of

the ratio of synchrotron satellites to the main peak height [1]. It can also be obtained by comparing the measured beam betatron motion with the theoretical curve [2, 3]. Compton back scattering is another way to measure the beam energy spread. Since the maximal energy of scattered photons is strictly coupled with the beam energy, the width of the maximal energy edge is determined by the energy spread.

Beijing Spectrometer (BESIII) is a general composite detector operating at Beijing Electron Positron Collider (BEPCII) [4, 5], whose physical goals involving charmonium physics, D -physics, spectroscopy of light hadrons and τ -physics. Accurate beam energy is essential in precise measurement, which can be an important source of systematic uncertainty in some analyses, e.g. τ mass measurement [6]. At BEPCII, σ_E is usually measured by scanning the width of narrow resonance, typically J/ψ and $\psi(2S)$. Once σ_E has been measured, it might be extrapolated to other center of mass (c.m.) energy \sqrt{s} , assuming it is proportional to s [7], $\sigma_E \propto s$. However, the status of accelerator might be different at energy far away from narrow resonances and different data taking period. The extrapolation may not be suitable, so more methods are needed to estimate the energy spread. Here we introduce two methods to measure the en-

ergy spread via the $e^+e^- \rightarrow \Lambda_c^+ \bar{\Lambda}_c^-$ process utilizing the data taken at BESIII. One method measures the c.m. energy spread based on threshold truncation effect, while another one estimates beam energy spread using spectra resolution. The c.m. energy is twice as the beam energy in an equal energy collision, therefore the spread of c.m. is larger than the beam energy spread by a factor of $\sqrt{2}$.

2 Measurement of center of mass energy spread based on threshold truncation

2.1 Method description

In e^+e^- collision, energy and momentum conservations guarantee that the c.m. energy \sqrt{s} of electron and positron system is equal to the invariant mass $M(X)$, where X denotes final particles. Therefore, we can measure \sqrt{s} with reconstructed particles in the detector. BESIII has used the $e^+e^- \rightarrow \mu^+\mu^-$ process to calibrate c.m. energies of a series of data samples [8]. However, for the case close to the threshold, the reconstructed invariance mass from final particles tends to have an average value larger than the mean of c.m. energy, since the collisions with energy below the production threshold don't contribute to the interested process, and this is likely due to energy spread. The larger energy spread σ_E , the more collisions below the threshold and thus higher average invariant mass.

So, σ_E could be determined if its relation with $M(X)$ is found. A general analytical relation is hard to obtain, since plenty of factors can impact on it. We use Monte Carlo (MC) simulation to extract the relation, taking influential factors into consideration, including the average \sqrt{s} , the energy spread σ_E , the behaviour of cross section line shape near the threshold, initial state radiation (ISR), final state radiation (FSR), the resolution of the detector and so on. After the simulation, the average $M(X)$ is generally not equal to the nominal energy \sqrt{s} , i.e. $\Delta_E = M(X) - \sqrt{s} \neq 0$, due to the energy spread and the threshold truncation effect. $M(X)$ can be obtained at a set of assumed σ_E to reveal the numerical relation between Δ_E and σ_E , which then can be used to determine σ_E when Δ_E is measured using experimental data.

2.2 Check with data taken at BESIII

At BESIII, \sqrt{s} measured with $\mu^+\mu^-$ events [8] is used as the standard value. The nominal energy of 4575 MeV is measured to be $4574.50 \pm 0.18 \pm 0.70$ MeV, where the first uncertainty is statistical and the second one systematic. However, the uncertainties can not reflect the energy spread since they mainly come from the statistics and the resolution of BESIII detector. To measure the energy spread at 4575 MeV, the $e^+e^- \rightarrow \Lambda_c^+ \bar{\Lambda}_c^-$ process is chosen because the energy is close to the production threshold which is 4572.96 ± 0.28 MeV. Λ_c^+ and $\bar{\Lambda}_c^-$ are unstable particles which decay immediately once they are produced. The process to reconstruct Λ_c^+ is $\Lambda_c^+ \rightarrow pK^-\pi^+$ and the charge conjugate (c.c.) channel for $\bar{\Lambda}_c^-$. To improve the statistics, only one Λ_c^+ or $\bar{\Lambda}_c^-$ is required in the reconstruction of the $e^+e^- \rightarrow \Lambda_c^+ \bar{\Lambda}_c^-$ process, and another $\bar{\Lambda}_c^-$ or Λ_c^+ is obtained from the recoiling information of the reconstructed one in e^+e^- center of mass system with its mass quoted from Particle Data Group (PDG) [9]. Then \sqrt{s} estimated from $\Lambda_c^+ \bar{\Lambda}_c^-$ pair is calculated with the invariant mass of total four-momentum, which will deviate from the mean value of collision energy \sqrt{s} as discussed above.

To estimate σ_E for the data, a toy MC is generated with assumptions:

- The cross section has a sharp step at the $\Lambda_c^+ \bar{\Lambda}_c^-$ threshold [10] pursuant to the Coulomb enhancement factor, $\pi\alpha/\beta$ [11], which cancels the phase space β and produces a sudden jump at threshold. BESIII cross section of the $e^+e^- \rightarrow \Lambda_c^+ \bar{\Lambda}_c^-$ process looks very similar to BaBar cross section of the $e^+e^- \rightarrow p\bar{p}$ process [12], which also shows a sharp step at threshold, followed by an almost flat behaviour and a cross section value close to the pointlike one, once the Coulomb enhancement factor has been taken into account.
- Energy spread is simulated by means of a Gaussian function, with variance σ_E .
- ISR photon γ is simulated according to [13]: $p(k) \sim \beta k^{\beta-1} (1 - k^{1-\beta} + 0.5k^{2-\beta})$, where k is the energy fraction taken by γ and $\beta = 4\alpha/\pi [\ln(E_{beam}/m_e) - 0.5]$ is the Touschek Bond factor
- The actual energy is $\sqrt{s} = 4574.50 \pm 0.72$ MeV,

as measured in Ref. [8]. The energy is sampled with a Gaussian assumption using the \sqrt{s} as the mean value and uncertainty as the width.

- \sqrt{s} reconstruction, in the case of $\Lambda_c^+ \bar{\Lambda}_c^-$ pair production, is simulated like a Gaussian function with width to be 9 MeV.
- All the parameters, like the Λ_c^+ mass, on the basis of PDG [9], sampled with Gaussian assumption in the simulation.

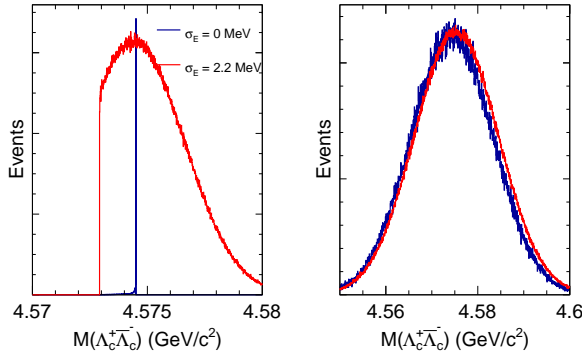


Fig. 1. (color online) The distribution of $M(\Lambda_c^+ \bar{\Lambda}_c^-)$ with (red) and without (blue) energy spread before (upper) and after (lower) detector reconstruction.

Based on above considerations, MC samples have been generated with σ_E to be 0 and 2.2 MeV. The comparison of the $M(\Lambda_c^+ \bar{\Lambda}_c^-)$ distributions between the two cases are shown in Fig. 1, which include the original distribution before interacting with detector and the reconstructed one using tracks from the detector. The reconstructed $M(\Lambda_c^+ \bar{\Lambda}_c^-)$ distribution of the case with energy spread is slightly shifted with respect to the one with $\sigma_E = 0$. The shift can be quantitatively described by the difference of the mean value or the peak value of the distributions.

The numerical relation between the energy spread σ_E and the spectra shift Δ_E is extracted via a series of toy MC generated with assumption σ_E from 1 to 4 MeV, 0.2 MeV step per MC sample. With each assumption of σ_E , Δ_E denotes the difference between the mean value of $M(\Lambda_c^+ \bar{\Lambda}_c^-)$ and the real energy, $\Delta_E = \langle M \rangle - \sqrt{s}_{\text{real}}$. The relationship between σ_E and Δ_E is reported in Fig. 2 and turns out to be almost linear in a low order approximation. Figure 2

also shows that magnitudes of σ_E and Δ_E are in the same order in our case that \sqrt{s} is ~ 1.5 MeV above threshold of $\Lambda_c^+ \bar{\Lambda}_c^-$.

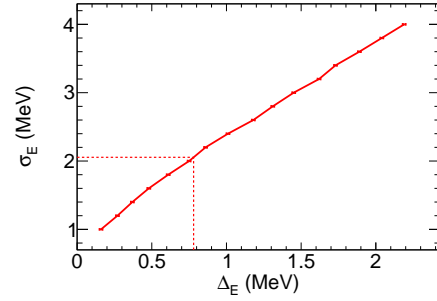


Fig. 2. The relation of σ_E and Δ_E from toy MC at $\sqrt{s} = 4574.50 \pm 0.72$ MeV. Dashed lines show the invariant mass shift of data and the corresponding energy spread.

To measure the energy spread of the data sample at $\sqrt{s} = 4575$ MeV, we need the shift of $M(\Lambda_c^+ \bar{\Lambda}_c^-)$. The invariant mass distribution of experimental data is obtained on basis of Λ_c^+ or $\bar{\Lambda}_c^-$ selected events and recoiling technique mentioned above, as shown in Fig. 3. The average invariant mass is measured to be $M(\Lambda_c^+ \bar{\Lambda}_c^-) = 4575.28 \pm 0.55$ MeV, which is about 0.78 MeV higher than \sqrt{s} measured on basis of the $\mu^+ \mu^-$ selected events [8]. Utilizing the relationship shown in Fig. 2, it is found that $\sigma_E = 2.1 \pm 1.1$ MeV. The energy spread is consistent with the value estimated from the extrapolation of the spread at J/ψ mass using the proportional relation between σ_E and s , which is $\sigma_E \approx 0.9$ MeV at J/ψ mass [14] and thus $\sigma_E \approx 2$ MeV at 4575 MeV.

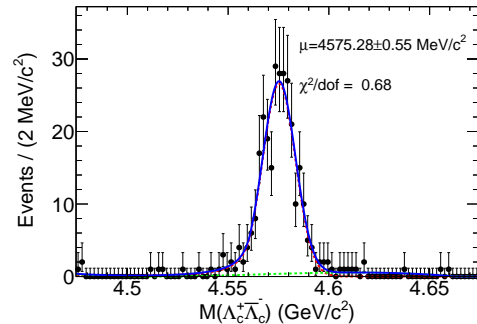


Fig. 3. (color online) $M(\Lambda_c^+ \bar{\Lambda}_c^-)$ distribution at 4575 MeV. Solid line is the fit result. Dashed lines represent signal (red) and background (green).

BESIII has also taken data at $\sqrt{s} = 4600$ MeV, which is a little far away from threshold of $\Lambda_c^+ \bar{\Lambda}_c^-$.

The invariant mass of $\Lambda_c^+ \bar{\Lambda}_c^-$ is extracted with the same method as used at $\sqrt{s} = 4575$ MeV, which is $M(\Lambda_c^+ \bar{\Lambda}_c^-) = 4599.3 \pm 0.2$ MeV as shown in Fig. 4. The value is consistent with that measured with $\mu^+ \mu^-$ event in Ref. [8], which is $4599.53 \pm 0.07 \pm 0.74$ MeV. There is no shift of $M(\Lambda_c^+ \bar{\Lambda}_c^-)$ at \sqrt{s} far away from threshold as expected.

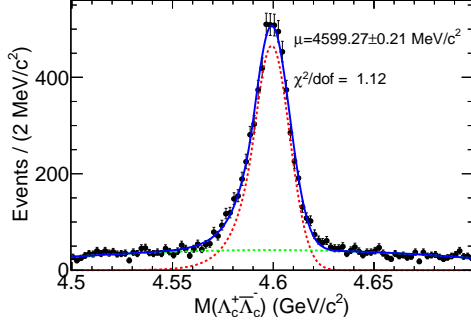


Fig. 4. (color online) $M(\Lambda_c^+ \bar{\Lambda}_c^-)$ distribution at 4600 MeV. Solid line is the fit result. Dashed lines represent signal (red) and background (green).

3 Measurement of beam energy spread based on the resolution of spectrum

3.1 method description

Many analyses in high energy physics strongly rely on MC simulation, which describes particle generation and detector response. If the detector is simulated very well, the spectra of reconstructed variables in MC simulation should be consistent with those in data. Generally, if we treat the beam energy as a single value to do the simulation, there will be some discrepancy between the spectra of data and MC simulation. Assuming the discrepancy comes from beam energy spread, if we taken the beam energy spread into consideration, the discrepancy should disappear. Therefore, we can use MC simulation to determine the beam energy spread.

3.2 Determination of beam energy spread

The $e^+ e^- \rightarrow \Lambda_c^+ \bar{\Lambda}_c^-$ process is chosen to do the energy spread measurement, and the beam-constrained mass M_{BC} is used to show the difference between data and MC simulation, where $M_{BC} =$

$\sqrt{E_{\text{beam}}^2/c^4 - |\mathbf{p}|^2/c^2}$ and \mathbf{p} is the momentum of Λ_c^+ or $\bar{\Lambda}_c^-$ reconstructed from final particles. The decay channels of Λ_c^+ and $\bar{\Lambda}_c^-$ are the same as the previous method.

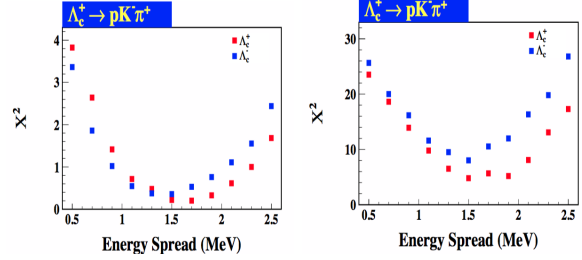


Fig. 5. (color online) The dependence of M_{BC} -fit χ^2 on beam energy spread value at $\sqrt{s} = 4.5745$ (left) and 4.5995 (right) GeV. The rectangular points represents χ^2 of each fit.

First, we generate a series of signal MC samples with different values of the beam energy spread, from 0.5 MeV to 2.5 MeV incremented by 0.2 MeV. Then, we extract M_{BC} distributions of these signal MC samples and use them to perform unbinned maximum likelihood fits on corresponding M_{BC} distributions in data directly. The χ^2 of each fit is obtained and used as indicator of the correctness of the beam energy spread value. Figure 5 shows the results at $\sqrt{s} = 4.5745$ and 4.5995 GeV. In order to find a reasonable beam energy spread value, the simple fits via the quadratic function on the χ^2 value at $\sqrt{s} = 4.5995$ GeV is performed. The fit function takes the form

$$\chi^2 = p_0 \cdot (x - p_1)^2 + p_2, \quad (1)$$

where x denotes the value of beam energy spread and p_1 is expected to be the nominal value of the beam energy spread. The fit results are shown in Fig. 6.

Note that the χ^2 values are not true data, since there is no uncertainties in them. Therefore the nominal uncertainty of p_1 , which is output by the fit is not available. Accordingly, we assign the deviation of the beam energy spread value, which enlarges corresponding χ^2 by 1.0, to be the uncertainty. Therefore, the fit of the positive mode gives that $p_1 = 1.618 \pm 0.254$ MeV while the negative mode results in $p_1 = 1.490 \pm 0.241$ MeV. The corresponding c.m. energy spread is $\sigma_E = \sqrt{2}p_1 = 2.1 \pm 0.3$ MeV, which is consistent with the first method.

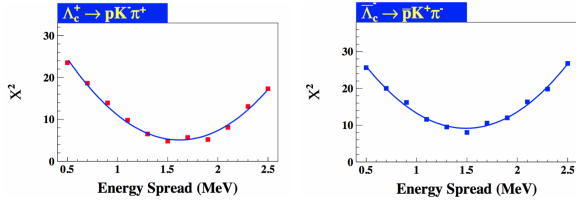


Fig. 6. (color online) The fit of χ^2 of the golden mode via the function $p_0 \cdot (x - p_1)^2 + p_2$, where the x represents the value of beam energy spread and p_1 is expected to be the nominal value of beam energy spread. The fit is performed on the χ^2 data which are extracted at $\sqrt{s} = 4.5995$ GeV, the blue solid lines represent the fit functions.

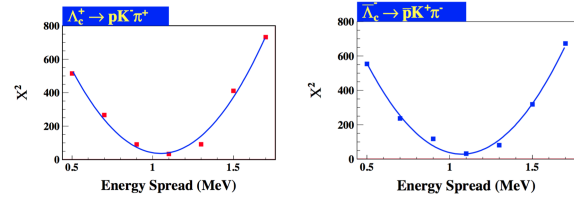


Fig. 7. (color online) The fit of χ^2 of the golden mode via the function $p_0 \cdot (x - p_1)^2 + p_2$, where the x represents the value of beam energy spread and p_1 is expected to be the nominal value of beam energy spread. The fit is performed on the χ^2 data which are extracted from the inclusive $\Lambda_c^+ \bar{\Lambda}_c^-$ MC samples. the blue solid lines represent the fit functions.

3.3 MC-based Input-Output check

In order to justify the method to determine the beam energy spread value, we performed a MC-based input-output check. The inclusive $\Lambda_c^+ \bar{\Lambda}_c^-$ MC samples are generated at $\sqrt{s} = 4600$ MeV with the beam energy spread assigned to be 1.1 MeV. First, we regard these samples as data and extract the M_{BC} distribution. Second, we use above signal shapes, in which the beam energy spread values are assigned from 0.5 MeV to 2.5 MeV, to perform unbinned maximum likelihood fits on the M_{BC} distribution of the inclusive $\Lambda_c^+ \bar{\Lambda}_c^-$ MC samples directly. Fit results are presented in Fig. 7. Similarly, the fit of the positive mode gives that $p_1 = 1.049 \pm 0.024$ MeV while the negative mode results in $p_1 = 1.073 \pm 0.025$ MeV. We assign the nominal value of beam energy spread, as well as its uncertainty, to be the weighted average of these two fitted values. This result is consistent with the input value, i.e. $\bar{p}_1 = 1.1$ MeV, if we take the systematic uncertainty of this method into account. Although the uncertainty is underestimated, the method we used to determine the beam energy spread value is justified.

4 Summary

Two methods are introduced to measure the energy spread of accelerator based on threshold truncation effect and spectrum resolution. For the first method based on threshold truncation effect, MC simulations have been performed to validate the method and extract the relationship between Δ_E and σ_E . The $e^+e^- \rightarrow \Lambda_c^+ \bar{\Lambda}_c^-$ process has been chosen to apply the method on BESIII data samples at $\sqrt{s} = 4575, 4600$ MeV. The energy spread is measured to be $\sigma_E = 2.1 \pm 1.1$ MeV at 4575 MeV, which is consistent with the extrapolation of energy spread at J/ψ mass. The measurement is only valid at \sqrt{s} very close to threshold which may limit the application of the method. In the second method which arises from spectrum resolution, χ^2 value as indicator shows the method works well, as verified by the MC input-output check. Both methods are reliable in the beam energy spread and c.m. energy spread measurement of accelerator physics.

5 Acknowledgement

References

- 1 T. Nakamura *et al.*, Chromaticity for energy spread measurement and for cure of transverse multi-bunch instability in the SPRING-8 storage ring, Proc. of the 2001 Particle Accelerator Conference, Chicago, p. 1972-1974.
- 2 V.V. Danilov, I.N. Nesterenko and E.A. Perevedentsev, Measurement of betatron coherent tune shifts and collective damping rates in BEP storage ring with the optical technique, Int. J. Mod. Phys. A (Proc. Suppl.) 2A (1993) 230.
- 3 N.A. Vinokurov *et al.*, The influence of chromaticity and cubic nonlinearity on kinematic of betatron oscillations, Preprint BINP 76-87, Novosibirsk (1976), in Russian.
- 4 BEPCII Group, BEPCII Design Report, IHEP- Proceedings, Aug. 2001.

-
- 329 5 M. Ablikim *et al.* (BESIII Collaboration), Nucl. Instrum. 338
 330 Meth. A **614**, 345 (2010). 339
 331 6 X.H. Mo, Nucl. Phys. B**169**, 132-139 (2007). 340
 332 7 Sands M., The Physics of electron positron storage rings, 341
 333 SLAC-121 (1979). 342
 334 8 M. Ablikim *et al.* (BESIII Collaboration), Chin. Phys. C 343
 335 **40**(6) 063001 (2016). 344
 336 9 C. Patrignani *et al.* (Particle Data Group), Chin. Phys. C 345
 337 **40**. 100001 (2016).
- 10 W.P. Wang, Cross section measurement of $e^+e^- \rightarrow \Lambda_c^+ \bar{\Lambda}_c^-$
 near threshold with BESIII, BESIII internal document.
 11 R. Baldini *et al.*, Eur. Rhys. J. A **39**, 315-321 (2009).
 12 B. Aubert *et al.* (BaBar Collaboration), Phys. Rev. D **73**,
 012005 (2006).
 13 K. Yu. Todyshev, arXiv:0902.4100, (2009)
 14 X.Y. Zhou, Measurement of J/ψ resonance parameters
 through energy scan, BESIII internal document.